

HOW TO OBTAIN HIGH QUALITY ELECTRON BUNCHES IN PRESENCE OF NORMAL CONDUCTING LINAC WAKEFIELDS

S. Di Mitri*, ELETTRA, Trieste, Italy

Abstract

The dynamics of electron beams involved in Free Electron Lasers (FELs) projects is an interplay between sources of 6-dimensional emittance dilution and methods of emittance preservation. Relatively long bunches are required for harmonic cascade seeded FELs in order to accommodate the timing jitter and the seed provided by the bunch itself at each stage of the cascade. A high quality is required from such electron beams (small transverse emittance and energy spread) together with a uniform distribution in time along the usable part of the bunch; non-linearity in the longitudinal phase space and in the transverse planes are also issues. A complex longitudinal phase space dynamics characterizes the study often in presence of by the Coherent Synchrotron Radiation (CSR) generated in magnetic compressors. This paper reviews specific problems related to the electron beam dynamics dominated by bunches of kA peak current and varying length (0.1 to 2 ps) in the presence of normal conducting linac wakefields. Methods implemented to minimize the 6-dimensional phase space degradation are discussed. Results of high beam quality performance are illustrated with particles tracking codes.

INTRODUCTION

This paper describes the degrading effects on the electron beam performance of wake fields present in normal conducting linacs for single pass FELs; in particular: (i) geometrical wake fields in accelerating structures [1–4]; (ii) Coherent Synchrotron Radiation (CSR) [5–8]; (iii) Longitudinal Space Charge (LSC) [9–12]. Their impact on the electron beam quality is discussed in terms of the properties relevant for Spontaneous Emission Self Amplified (SASE) [13–15] and seeded [16–19] FELs.

All the mentioned wake fields couple the 6-dimensional particle dynamics by putting some conflicting constraints on the design of the beam delivery system dedicated to the formation of electron bunches. This paper reviews some strategies for the machine design to compensate the emittances growth and improve the beam quality. The conclusions demonstrate the validity of manipulation techniques to control the electrons 6-dimensional phase space to unprecedented levels.

WAKE FIELDS AFFECTING THE ELECTRON BEAM QUALITY

In order to make the FEL process more efficient and the undulators chain reasonably short, the electron beam quality has to be characterised by high peak current, small transverse emittance, small energy spread. Due to the cooperative FEL process, priority is given to the slice beam quality.

Longitudinal phase space

Short range longitudinal wake fields generated by relatively short bunches with $\sigma_z \ll a$, being σ_z the bunch length and a the beam pipe radius, travelling into periodical structures induce a maximum FWHM relative energy loss [20]:

$$\frac{\Delta\gamma}{\gamma} = \frac{eW_0QL}{E_f} \quad (1)$$

which is valid in the approximation $(\sigma_z/s_0)^{1/2} \ll 1$ with s_0 the characteristic parameter of the structure.

Assuming a linear energy gain in the linac, (1) shows that the impact of very long accelerators can be comparable to that of smaller machines. For example, the energy loss in the LCLS Linac 3 relative to the final average energy is about 0.5% [21], while that in the FERMI Linac 4 is 1.4% [22]. Off-crest acceleration is then needed to reduce the induced energy chirp below the FEL threshold and to re-establish the linearity in the longitudinal phase space.

With an appropriate positioning of the magnetic chicanes, longitudinal wake fields acting in the last part of the linac work for free to cancel the linear energy chirp required by the compression. In this way the chicane momentum compaction can be relaxed, thus reducing the influence of CSR, while using larger energy chirps.

Even after cancellation of the linear contribution, residual higher order energy chirps affect the final beam quality. A quadratic chirp $D(2) = d^2E/d^2z$ increases the correlated energy spread, thus reducing the SASE FEL gain. It also enlarges the bandwidth of a High Gain Harmonic Generation (HG) FEL to unwanted levels, corrupting the goal of producing a Fourier transform limited signal with narrow bandwidth of the order of few meV [23–25]. Figures 1–4 illustrate this topic comparing two cases with different values of the quadratic energy chirp.

*simone.dimitri@elettra.trieste.it

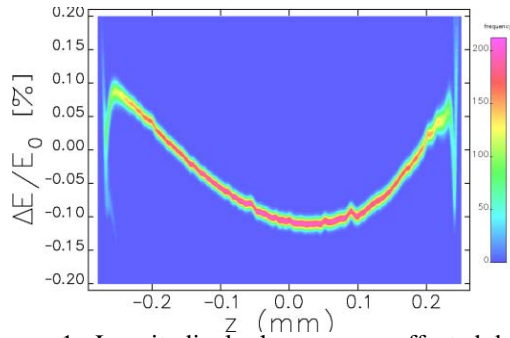


Figure 1. Longitudinal phase space affected by 0.9 MeV/ps² quadratic energy chirp.

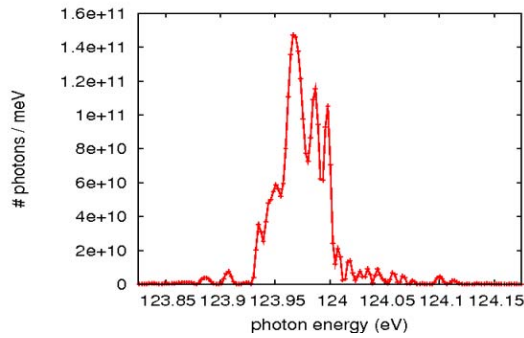


Figure 2. Spectral bandwidth of 40 meV FWHM generated by the electron bunch in Figure 1 through FERMI HGFG with fresh bunch technique at 10 nm.

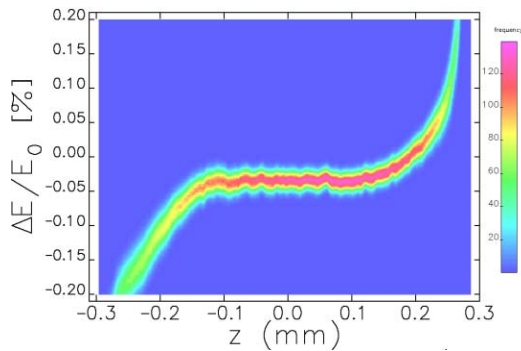


Figure 3. Longitudinal phase space affected by a reduced 0.5 MeV/ps² quadratic energy chirp.

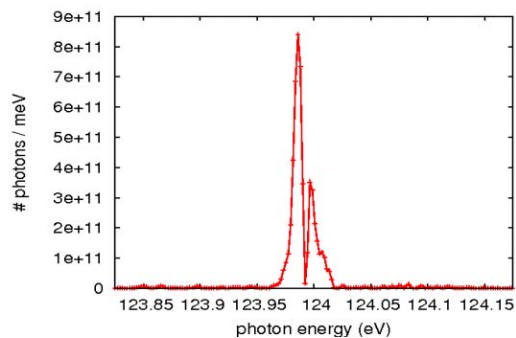


Figure 4. Spectral bandwidth of 10 meV FWHM generated by the electron bunch in Figure 3 through FERMI HGFG with fresh bunch technique at 10 nm.

Phase spaces and bandwidths were produced respectively by mean of Elegant [26] and Genesis [27].

The use of sextupoles [28] and of a high harmonic cavity [29–31] (also called “linearizer”) to compensate the quadratic chirp is well-established. Nevertheless, it was also shown that a residual cubic chirp in the compression process can have a large impact on the final current profile [32].

Current profile

SASE FELs generally require a high peak current (kAs) in the bunch core, while HGFG FELs desire a uniform current distribution along the whole bunch, especially if based on fresh bunch injection technique. Even if with different purposes, both the first and the latter need a control of the final current distribution. A proper manipulation of the cubic energy chirp $D(3) = d^3E/d^3z$ is useful to maximize the current along the bunch and to avoid current spikes at the bunch edges. In fact, they are related to several dangerous effects: (i) introduce nonlinearity in the phase space (i.e., bifurcations); (ii) attract particles reducing the current in the bunch core; (iii) induce CSR instability at shorter wavelength than the bunch length; (iv) wake field excited by a leading edge spike may cause additional energy spread in the undulator vacuum chamber.

Transverse emittance

Apart from SC forces at low energy, slice emittance is directly affected by transverse CSR forces [6,33,34]. A coherent behaviour of the emitted radiation has been also observed at wavelength smaller than the bunch length [12,35]; due to the interplay of LSC and CSR on wavelengths which are a fraction of the bunch length, microbunching instability (μBI) [36–40] leads to phase space fragmentation and to slice emittance growth.

The projected emittance of high charge, short bunches is indirectly affected by CSR emitted on the scale of the bunch length [41–43]. Due to the absence of stochastic processes, the slices lateral offset can be cancelled through a $-I$ transport matrix between two identical dispersive regions [44].

The transverse wake field contributes to the projected emittance growth by mean of the induced beam break up (BBU) instability [45,46]. The coupling between the electron bunch and the wake field at a given energy can be estimated by mean of the following dimensionless parameter [47]:

$$\varepsilon_r = \frac{4\pi\varepsilon_0 W_0 l_b L^2 I_{pk}}{\gamma_i I_A} \quad (2)$$

It multiplies the resonant term acting on the transverse motion of the slices centroid, thus it should be made as small as possible.

CUBIC ENERGY CHIRP

The sign of the cubic energy chirp in the photo-injector (PI) is mainly determined by the SC force and,

according to the present simulations, it is always negative for a flat-top charge distribution (bunch head on the left side of phase space) [48]. After the interaction with longitudinal wake fields, this sign is reversed at the entrance of the second compressor, enhancing the energy-position correlation of the bunch edges w.r.t the core. The edges are there over-compressed producing current spikes. On the contrary, a negative cubic chirp at the chicane provides under-compression of the edges. This mechanism is illustrated in Figure 5, where the longitudinal phase space and the corresponding current profile generated by LiTrack [49] are shown.

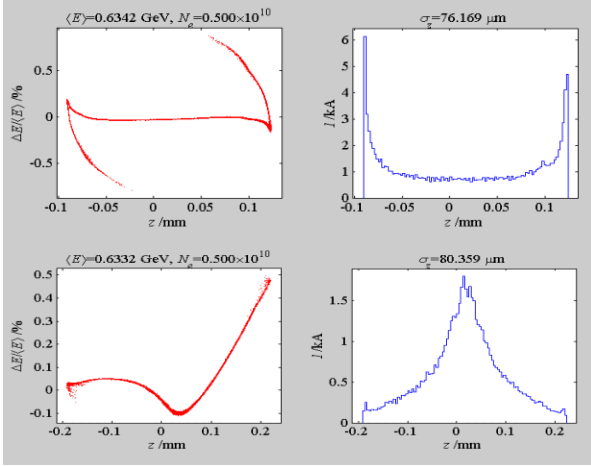


Figure 5. Longitudinal phase space (left) and current profile (right) at the end of the FERMI Linac. Cubic chirp at the PI is $-3.9 \times 10^{-4} \text{ mm}^{-3}$ at top and $8.1 \times 10^{-4} \text{ mm}^{-3}$ at bottom.

Voltage and phase of the high harmonic cavity allow to control the cubic chirp in the following transport line that is the final current profile. For a 1-stage compression the following parameters are defined: $k=2\pi/\lambda_{rf}$ is the RF wave number and λ_{rf} is the RF wavelength; U_0 is the voltage amplitude of a first linac accelerating on-crest; U_1 is the amplitude of a second linac with off-crest acceleration at phase ϕ_1 (referred to the crest of the RF wave); U_4 and ϕ_4 are the amplitude and phase of the 4-th harmonic cavity. Thus, the third derivative of the energy gain is:

$$U''_{(s=0)} = -k^2 U'_{(s=0)} + \frac{15}{4} k^3 (U_0 + U_1 \cos(\phi_1)) \tan(\phi_4) \quad (3)$$

The quadratic chirp is cancelled if:

$$U_4 = -\frac{U_0 + U_1 \cos(\phi_1)}{16 \cos(\phi_4)} \quad (4)$$

(3) and (4) define the space where parameters of the harmonic cavity can be moved in order to linearize the longitudinal phase space up to the 3rd order.

REVERSE TRACKING

Due to the complexity of the interplay of SC, longitudinal wake fields and higher order energy chirps, it is not obvious to control simultaneously

longitudinal phase space and current profile. In addition, it was demonstrated [50] that the linearizer can be used to relax until an order of magnitude the sensitivities of the final beam properties to the linac phase and voltage. Unfortunately, this technique assumes a negligible effect of the cubic chirp on the longitudinal beam dynamics and considers it a free parameter.

The reverse tracking [32] suggests how to improve the global quality of the longitudinal phase space for a given configuration of the wake potential, eventually leaving the linearizer free to be moved for jitter purposes. It applies to ultra-relativistic particles and is based on the assumptions of no stochastic processes in the beam transport and of negligible energy loss from CSR. CSR with wavelength in the range of the bunch length can be neglected in presence of an appropriate shielding [32,51,52] of the vacuum chamber. Moreover, the induced energy loss is relatively small for long bunches.

Within these approximations, the equations of motion can be reversed and a unique solution exists. The density distribution obtained at the beginning of the linac will automatically compensate all the effects perturbing the beam dynamics in the forward tracking, like RF curvature, wake fields and higher order optics.

It is clear this method calls the beam shaping at the photo-cathode to be a fundamental contribution to the final beam quality. For the FERMI specific case [32], a final beam with a flat current profile and a linear phase space corresponds to an initial beam with a ramped current profile (see, Figure 6).

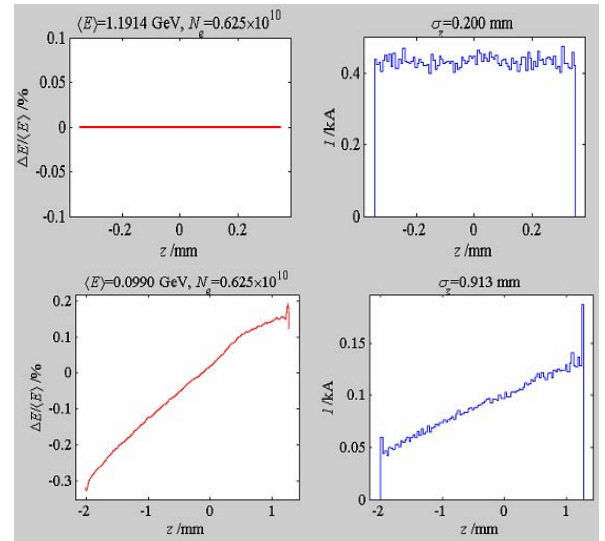


Figure 6. Top, electron beam desired at the undulators' entrance. Bottom, electron beam required at the PI end. LiTrack [49] output.

The approximate prediction of the reverse tracking was confirmed by the forward tracking, obtaining the phase space in Figure 3. In addition, it was proved that the convolution of the longitudinal wake function with

a ramped particle distribution results in a mostly linear wake potential (see, Figure 7), while an initial parabolic current profile brings nonlinear contributions to the phase space.

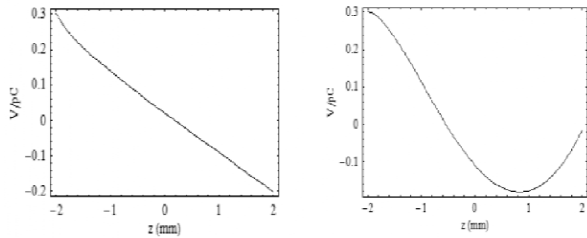


Figure 7. Longitudinal wake field generated in the FERMI Linac 4 resulting from the convolution of the wake function with a particles distribution characterized by a ramped current profile (left) and a parabolic one (right).

BEAM SHAPING AT THE PHOTO-INJECTOR

As discussed before, in presence of wake fields the initial electron density distribution plays an important role in formation of the electron bunches at the end of the accelerator [53–55]. As for the FERMI case, the LSC field at the cathode was investigated [56], since it is mainly responsible for blowing out the particles. Figure 8 shows the desired current profile at the cathode and the evolved charge distribution at the injector exit (at 100 MeV) for a 0.8 nC bunch.

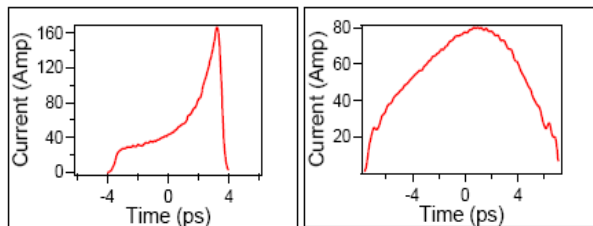


Figure 8. Ramped current distribution just after the cathode (left) and at the injector exit (right) for a 0.8 nC bunch.

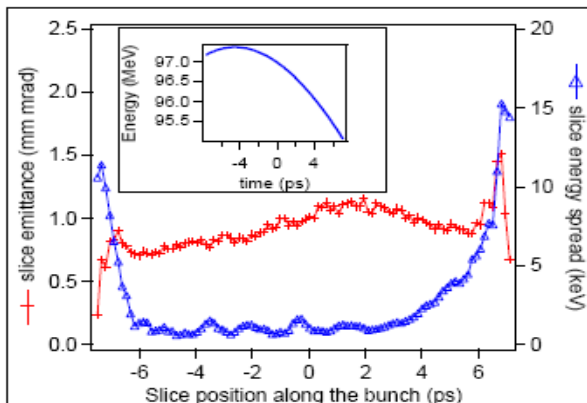


Figure 9. Slice emittance and slice energy spread along the bunch at the exit of the injector. $\epsilon_{xn,80\%} = 1.2$ mm mrad. Inside plot: longitudinal phase space including longitudinal wake fields. Head is on the left.

Since each longitudinal slice of the beam contains a differing amount of charge, each one evolves in a different way from the other. Thus, the so-called Ferrario’s working point [57] can be only approximately adopted for the emittance compensation. Figure 9 shows the resulting slice emittance and the slice energy spread for the bunch in Figure 8 at the injector exit; results were produced through the GPT code [58].

BBU SUPPRESSION

BBU instability induces a lateral deviation of the bunch tail w.r.t. the head axis. The persistence of such oscillations tend to transform the temporal coordinate into the transversal one, thus inducing projected emittance dilution. A “banana” shape in the (t, x) and (t, y) plane is assumed by the electron bunch [59]; it makes a large part of the bunch travelling with a trajectory offset in the undulator. This fact reflects into an optical mismatch in the undulators and can also induce an effective K-value for the tailing particles different from the nominal one. The impact of a launching error of the bunch in an undulator for SASE FEL was studied and experimentally observed [60]. The off-axis motion in the device leads to power reduction and bandwidth enlargement because of the processes addressed above.

As for seeded FELs, if the bunch tail deviation is sufficiently larger than the beam size, it causes a missed overlap between the seeding laser and the bunch in the undulator, thus reducing the emitted photon pulse length and the peak power [61]. Figure 10 illustrates the horizontal banana shape exiting from the FERMI Linac (Elegant simulation) and a schematic of the seeding laser overlapping the beam.

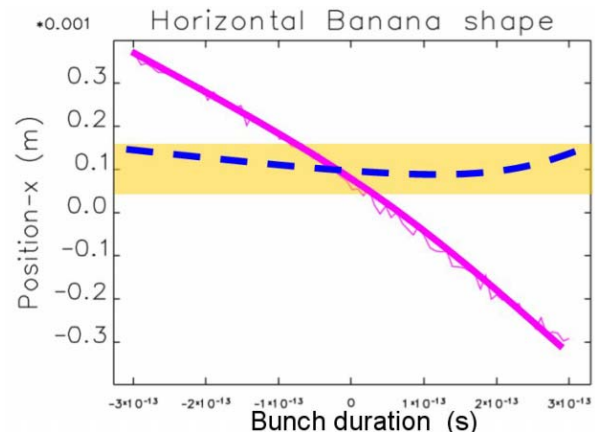


Figure 10. Horizontal banana shapes induced in the FERMI Linac. Bunch head is on the left. The solid curve shows a tail deviation 8 times larger than the 80 μ m rms beam size. The dashed one corresponds to a different trajectory in the Linac for which the tail deviation is within the rms beam size. The superimposed rectangle sketches the seeding laser and points out its overlap with the bunch in the two cases.

Figure 11 represents the dependence of peak power and phase shift for the FERMI FEL-1 scheme at 40 nm on the off-axis displacement error of the electron bunch at the undulator entrance [61].

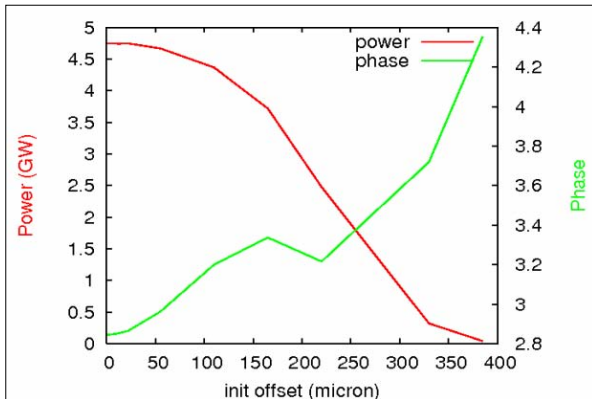


Figure 11. Effect of an off-axis displacement error of the electron bunch at the undulator entrance on peak power (decreasing with offset) and phase shift (increasing with offset) for FERMI FEL-1 HGHG scheme tuned at 40 nm. Seeding laser spot size is here assumed to be 210 μm .

In single pass FELs the BBU instability can be suppressed through trajectory bumps [59,62]. This technique looks for a “golden trajectory” for which all the kicks generated by the transverse wake field compensate each other and the banana shape is finally cancelled. Dashed curve in Figure 10 shows a compensated banana shape which maximizes the overlap with the seeding laser; the solid curve is the banana shape obtained in absence of bumps.

Since the bump is a local method of correction, it depends on the particular condition of operation at its location. For this reason, the sensitivity of the bump to the trajectory jitters has to be checked and made sufficiently small [59].

Reducing the average β -function along the linac is also useful since its square is proportional to the induced relative emittance growth [63]. On the other hand, in a FODO lattice the quadrupole strength $k \sim 1/\beta$ and the trajectory affected by errors $u_{\text{err}} \sim k\sqrt{\beta}$. Thus, lowering the β -function increases the sensitivity to the elements misalignment.

LOW CHARGE OPTION

The previous paragraphs describe techniques of electron beam manipulation in order to compensate the wake fields effects. Now a more general prescription of low charge beam production is exposed to minimize the wake fields once the compression factor, the final peak current and the final average energy are fixed.

The curves in Figure 12 represent the loss factor of a Gaussian charge distribution travelling in one accelerating structure of the FERMI Linac 4 vs. the rms bunch length; each curve is drawn for a given peak current (upper curve is at higher current), which is the

parameter of interest for the FEL. Dots represent a 0.6 nC charged beam which is compressed twice (dots move from right to left) by a total factor of 15; triangles show the same dynamics for a 0.3 nC charged beam.

Due to the monotonic behaviour of the wake functions in the range of bunch length considered, a bunch with lower charge always suffers from a minor energy loss w.r.t. the higher charge option (look at the height of the yellow and orange bars). Obviously, for a fixed peak current a shorter bunch is required from the PI and will be provided at the end of the accelerator.

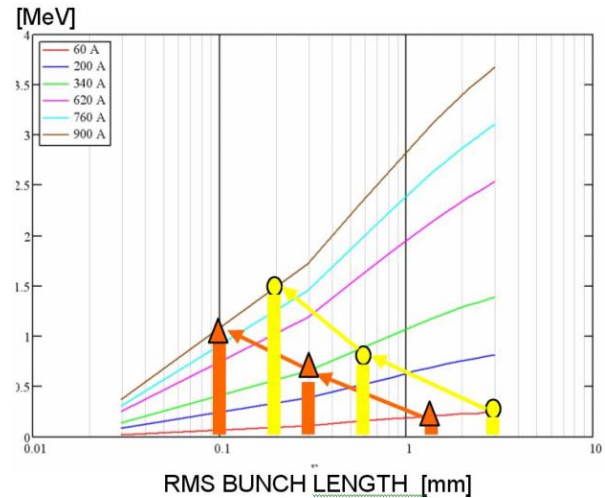


Figure 12. Loss factor in the FERMI Linac 4 accelerating structure vs. rms bunch length (a Gaussian charge distribution is assumed). Dots refer to the 0.6 nC electron bunch in a 2-stage linear compression (from right to left, the peak current increases as the bunch length decreases). Triangles refer to the 0.3 nC case.

Limitations to the shorter bunch length achievable are: (i) CSR instability; in the steady state approximation the induced rms energy spread $\sigma_{\delta, \text{CSR}} \sim I/\sigma_z^{1/3}$ [5]. This has an impact in terms of both energy modulation and brightness degradation [56]; (ii) timing jitter, especially for HGHG FELs with fresh bunch injection technique; the final bunch has to be sufficiently long in order to accommodate the timing jitter of the electron bunch w.r.t. the seeding laser.

A 0.2 nC low charge solution has been recently adopted by LCLS [64] instead of the 1.0 nC initially chosen; their dynamics is compared in Figure 13; there the low charge bunch shows an improvement in the longitudinal phase space linearity, a reduction of the current spikes at the bunch edges and a suppression of the BBU instability up to 10% of emittance growth. Reduction of the emittance from 1.2 to 0.85 mm mrad allows to obtain the same saturation length of the 1.0 nC case with a lower peak current (2.1 kA instead of 3.4 kA).

In some cases, a low charge option can also minimize the impact of CSR and SC forces on the

transverse emittance. For the TESLA-XFEL, a low charge working point [65] of 0.25 nC was found with a good compromise between the slice emittance growth, due to stronger CSR transverse forces at shorter bunch length, and the preservation of the projected emittance, which is no longer affected by the optical mismatch generated by SC forces at low energies.

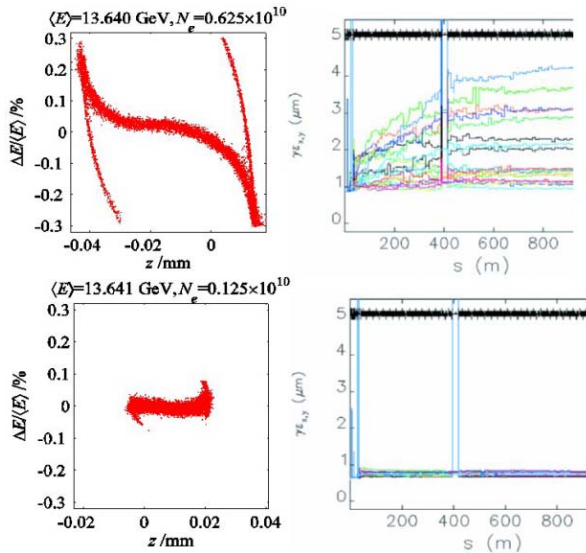


Figure 13. Longitudinal phase space (left plots) and transverse normalised projected emittance (right plots) in LCLS for the 1.0 nC charged bunch at top and for the 0.2 nC charged bunch at bottom.

LANDAU DAMPING

In the last 10 years microbunching instability (μBI) has been extensively studied and recently observed in experiments. The gain of the instability was calculated analytically in the 2-dimensional approximation [37,38]. Numerical solution was obtained including Landau damping from the beam finite emittance [39].

According to the linear theory, the longitudinal Landau damping can be made more effective by increasing the relative energy spread and the compression factor, like in a 1-stage compression. In fact, when adopting a 2-stage compression, analytical estimations confirmed by simulations demonstrate the fundamental role of the second compressor in the development of the μBI : it transforms all the LSC induced energy modulation accumulated in the upstream linac into density modulation; this effect sums to the enhancement of the density modulation already developed by the first compressor.

Figure 14 compares the spectral gain function of the 2-stage and of the 1-stage compression in the FERMI Linac [66]. The maximum of the instability gain is reduced by a factor 100 in the latter case.

The 1-stage compression is a pretty attractive solution but forces a very short bunch to travel along a large part of the linac; as a consequence, linearity of the longitudinal phase space is strongly affected by wake fields. This problem could be overcome by

applying the reverse tracking to the single compression scheme [67].

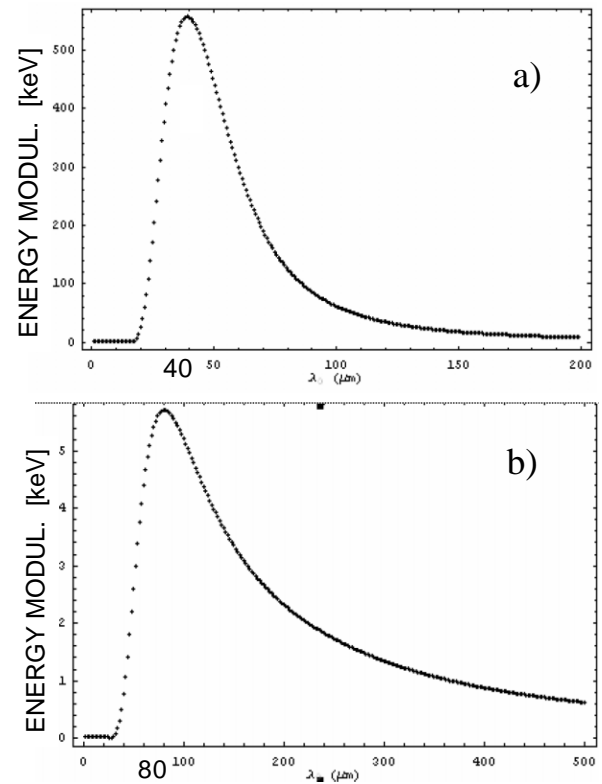


Figure 14. Spectral gain function of the microbunching instability in the FERMI Linac in case of double (a) and single (b) compression. Calculation is based on the 2-dimensional model for CSR and LSC in the linear approximation. μBI starts from realistic shot noise.

A 2-stage magnetic compression is generally associated with a laser heater at low energy for the reasons addressed above. This tool was proposed [9] to suppress the instability by increasing the relative energy spread just before the compression; on the other hand, its final value has to be still maintained below the FEL threshold. This is not obviously reached in low and medium energy machines and becomes more stringent for multi-stage harmonic cascade FELs.

Figure 15 shows the final slice energy spread as function of the energy spread induced by the laser heater in FERMI. μBI is supposed to start from shot noise in the initial density distribution. Figure 15 allows a comparison between the 2-dimensional analytical solution and the simulation of a Vlasov solver [68]. A Vlasov solver (see also [69]) avoids the problem of numerical noise in the simulation and automatically includes a nonlinear evolution of the instability which manifests itself in a folded phase space. This is not considered in the linear theory. Figure 15 shows a discrepancy in the results obtained with the two methods. Such studies, of general interest, are still in progress; the preliminary results indicate

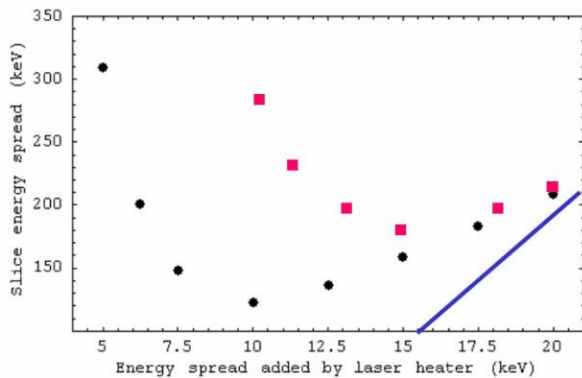


Figure 15. Rms slice energy spread in the final bunch for FERMI vs. the rms energy spread added by the laser heater at 100 MeV. Dots are the analytical prediction; squares are the results of the Vlasov solver. The solid line shows the expected energy spread in absence of any collective effect assuming a compression factor of 10 in linear approximation.

that the final prediction can often depend on details of the calculation.

CONCLUSIONS

The main effects on the electron beam quality by accelerating structures wake fields, CSR and LSC were reviewed in terms of the most relevant beam parameters for single pass FELs. This analysis points out the correlations between the 3 degrees of freedom of the electron dynamics in the accelerator generated by the wake fields.

A double magnetic compression results to be a suitable compromise to minimize instabilities induced by SC, longitudinal and transverse wake fields; at the same time, longitudinal wake field in the linac structures can be used to reduce the CSR effect in the second chicane.

Simultaneous control of the linearity in the longitudinal phase space and of the current profile can be achieved, under some approximations, by following the predictions of the reverse tracking. This technique forces the electron density distribution at the injector to cover an important role in formation of the electron bunches at the end of the accelerator. PI laser can be used to provide such suitable distribution for given wake potential; at the same time, special care has to be taken as for the emittance compensation scheme for unusual charge distributions exiting the photo-cathode.

A general prescription of low charge beam generation was investigated. Simulations demonstrate that it brings several advantages in achieving a high beam quality; essentially, it reduces the effects of the accelerating structures wake fields, allows a compromise between slice and projected emittance growth, maximizes the current along the bunch.

Suppression of the microbunching instability was treated by means of the single compression scheme, eventually joined with the reverse tracking, and of the laser heater. Implementation of the instability in 6-

dimensional full s2e simulations is still work in progress. Nevertheless, recent results demonstrate the importance of shot noise as a driving term.

REFERENCES

- [1] K. Bane, M. Sands, "Wakefields of very short bunches in an accelerating cavity", SLAC-PUB-4441 (1987).
- [2] K. Bane, "Short-range dipole wakefields in accelerating structures for the NLC", SLAC-PUB-9663, LCC-0116 (2003).
- [3] P. Craievich, T. Weiland, I. Zagorodnov, "The short-range wakefields in the BTW accelerating structure of the ELETTRA Linac, NIM A, **558**, 58 (2006).
- [4] P. Craievich et al., "The accelerator design study for the FERMI FEL", ST/F-TN-05/01 (2005).
- [5] Y. Derbenev, J. Rossbach, E. Saldin, V. Shiltsev, "Microbunching radiative tail-head interaction", TESLA-FEL 95-05 (1995).
- [6] Y. Derbenev, V. Shiltsev, "Transverse effects of microbunch radiative interaction", SLAC-PUB-7181 (1996).
- [7] E. Saldin, E. Schneidmiller, M. Yurkov, "On the coherent radiation of an electron bunch moving in an arc of a circle", NIM A, **398**, 373 (1997).
- [8] M. Borland et al., NIM A, **483**, 268 (2002).
- [9] E. L. Saldin, E. A. Schneidmiller, M. V. Yurkov, DESY Report No. TESLA_FEL-2003-02 (2003).
- [10] T. Shaftan, Z. Huang, "Experimental characterization of a space charge induced modulation in high-brightness electron beam", PRST-AB, **7**, 080702 (2004).
- [11] K. Tian et al., "Experimental observation of longitudinal space-charge waves in intense electron beams", PRST-AB, **9**, 014201 (2006).
- [12] M. Huning, P. Piot, H. Schlarb, "Observation of longitudinal phase space fragmentation at the TESLA test facility free-electron laser", NIM A, **475**, 348 (2001).
- [13] S. Milton et al., Science **292**, 2307 (2001)
- [14] C. Pellegrini, NIM A, **445**, 124 (2000).
- [15] A. Tremaine et al., PRL **88**, 204801 (2002).
- [16] R. Bonifacio, L. De Salvo Souza, E.T. Scharlemann, NIM A, **296**, 787 (1990).
- [17] I. Ben-Zvi, K. M. Yang, L. H. Yu, NIM A, **318**, 726 (1992).
- [18] L.H. Yu et al., Science, **289**, 932 (2000).
- [19] G. Penn et al., Proc. of EPAC 2004, Lucern, Switzerland (2004).
- [20] R. Gluckstern, PRD, **39**, 2780 (1989).
- [21] "LCLS CDR", SLAC-R-593 (2002).
- [22] P. Craievich, S. Di Mitri, "Electron beam simulations for the FERMI project at Elettra", Proc. of FEL 2004, Trieste, Italy.
- [23] S. G. Biedron, S.V. Milton, and H.P. Freund, NIM A **475**, 401 (2001).

- [24] T. Shaftan et al., Phys. Rev. E, **71**, 046501 (2005).
- [25] W. Fawley, G. Penn, "Thoughts on Spectral Broadening Effects in FERMI and other FEL's Based upon Seeded Harmonic Generation", ST/F-TN-06/07 (2006).
- [26] M. Borland, APS LS-287 (2000).
- [27] <http://corona.physics.ucla.edu/~reiche/>
- [28] R. England et al., PRST-AB, **8**, 012801 (2005).
- [29] P. Emma, "X-band RF harmonic compensation scheme for linear bunch compression in the LCLS", LCLS-TN-01-1 (2001).
- [30] K. Flottmann, T. Limberg, P. Piot, "Generation of ultrashort electron bunches by cancellation of nonlinear distortions in the longitudinal phase space", TESLA FEL 2001-06.
- [31] P. McIntosh et al., "Realization of an x-band rf system for LCLS", Proc. of PAC 2005, Knoxville, Tennessee
- [32] A. Zholents et al., "Formation of electron bunches for harmonic cascade x-ray free electron lasers", Proc. of EPAC 2004, Edinburgh, Scotland, UK.
- [33] R. Talman, "Novel relativistic effect important in accelerators", PRL, **56**, **14**, 1429 (1986).
- [34] B. Carlsten, T. Raubenheimer, "Emittance growth of bunched beams in bends", PRE, **51**, **2**, 1453 (1995).
- [35] T. Limberg, P. Piot, E. Schneidmiller, "An analysis of longitudinal phase space fragmentation at the TESLA test facility", NIM A, **475**, 353 (2001).
- [36] M. Dohlus, A. Kabel, T. Limberg, "Uncorrelated emittance growth in the TTF-FEL bunch compression sections due to coherent synchrotron radiation and space charge forces", Proc. EPAC 1998, Stockholm, Sweden.
- [37] E. Saldin, E. Schneidmiller, M. Yurkov, "Klystron instability of a relativistic electron beam in a bunch compressor", NIM A, **490**, 1 (2002).
- [38] Z. Huang, K. Kim, "Formulas for coherent synchrotron radiation microbunching in a bunch compressor chicane", PRST-AB, **5**, 074401 (2002).
- [39] S. Heifets, S. Krinsky, G. Stupakov, "Coherent synchrotron radiation instability in a bunch compressor", PRST-AB, **5**, 064401 (2002).
- [40] Z. Huang et al., "Suppression of microbunching instability in the linac coherent light source", PRST-AB, **7**, 074401 (2004).
- [41] M. Dohlus, T. Limberg, "Emittance growth due to wake fields on curved bunch trajectories", NIM A, **393**, 494 (1997).
- [42] P. Emma, R. Brinkmann, "Emittance dilution through coherent energy spread generation in bending systems", SLAC-PUB-7554 (1997).
- [43] P. Emma, "Issues and challenges for short pulse radiation production", Proc. of EPAC 2004, Lucerne, Switzerland.
- [44] D. Douglas, "Suppression and enhancement of CSR-driven emittance degradation in the IR-FEL driver", JLAB-TN-98-012 (1998).
- [45] J. Delayen, PRST-AB, **6**, 084402 (2003).
- [46] J. Delayen, PRST-AB, **7**, 074402 (2004).
- [47] P. Craievich, S. Di Mitri, "Emittance growth due to short-range transverse wakefields in the FERMI linac", Proc. FEL 2005, SLAC, California, USA.
- [48] G. Penco, private communications.
- [49] K. Bane P. Emma, Proc. PAC 2005, Knoxville, Tennessee, (2005).
- [50] M. Dohlus, T. Limberg, "Bunch compression stability dependence on RF parameters", Proc. of FEL 2005, SLAC, California.
- [51] J. Nodvick, D. Saxon, "Suppression of coherent radiation by electrons in a synchrotron", PR, **96**, **1** (1954).
- [52] R. Li, C.L. Bohn, J.J. Bisognano, Proc. Particle Accelerator Conference 1997, 1644 (1997).
- [53] C. Limborg-Deprey, P. R. Bolton, LCLS-TN-04-16.
- [54] C. Limborg-Deprey, Proc. of FEL 2005.
- [55] H. Loos et al., Proc. of FEL 2005.
- [56] S. Lidia, G. Penco, M. Trovo', "Optimization studies of the FERMI@Elettra photoinjector", Proc. of EPAC 2006, Edinburgh, Scotland.
- [57] M. Ferrario et al., SLAC-PUB-8400 (2000)
- [58] S.B. Van der Geer et al., <http://www.pulsar.nl/gpt/index/html>.
- [59] P. Craievich, S. Di Mitri, "Beam break-up instability in the FERMI@Elettra linac", Proc. of EPAC 2006, Edinburgh, Scotland, UK.
- [60] G. Andonian et al., "Observation of anomalously large spectral bandwidth in a high-gain self-amplified spontaneous emission free-electron laser", PRL, **95**, 054801 (2005).
- [61] G. De Ninno, W. Fawley, G. Penn, "Effect of Off-Axis Displacement Errors on FEL-1", ST/F-TN-06/01 (2006).
- [62] P. Tenenbaum, SLAC-TN-04-038 (2004).
- [63] K. Bane, Proc. of EPAC 2004, Lucerne, Switzerland.
- [64] P. Emma et al., "An optimized low-charge configuration of the linac coherent light source", Proc. of PAC 2005, Knoxville, Tennessee.
- [65] T. Limberg et al., "Optimized bunch compression system for the European xfel", proc. Of PAC 2005, Knoxville, Tennessee, USA.
- [66] A. Zholents, ST/F-TN-05/15
- [67] A. Zholents, private communications
- [68] M. Venturini, R. Warnock, and A. Zholents, "Development of a 2D Vlasov Solver for Longitudinal Beam Dynamics in Single-Pass Systems", LBNL Report LBNL-60513.
- [69] G. Bassi, J. A. Ellison, R. Warnock, "Progress on a Vlasov treatment of coherent synchrotron radiation from arbitrary planar orbits", Proc. of PAC 2005.